

Evaluating Privacy Leakage in Split Learning

Xinchi Qiu,¹ * Ilias Leontiadis² Luca Melis² Alex Sablayrolles² Pierre Stock²

¹ University of Cambridge
² Meta

Abstract

Privacy-Preserving machine learning (PPML) can help us train and deploy models that utilize private information. In particular, on-device machine learning allows us to avoid sharing raw data with a third-party server during inference. On-device models are typically less accurate when compared to their server counterparts due to the fact that (1) they typically only rely on a small set of on-device features and (2) they need to be small enough to run efficiently on end-user devices. Split Learning (SL) is a promising approach that can overcome these limitations. In SL, a large machine learning model is divided into two parts, with the bigger part residing on the server side and a smaller part executing on-device, aiming to incorporate the private features. However, end-to-end training of such models requires exchanging gradients at the cut layer, which might encode private features or labels. In this paper, we provide insights into potential privacy risks associated with SL. Furthermore, we also investigate the effectiveness of various mitigation strategies. Our results indicate that the gradients significantly improve the attacker’s effectiveness in all tested datasets reaching almost perfect reconstruction accuracy for some features. However, a small amount of differential privacy (DP) can effectively mitigate this risk without causing significant training degradation.

1 Introduction

On-device machine learning (ML) involves training and/or deploying models directly on the device without relying on cloud-based computing. This approach brings several benefits to the table, including increased privacy, reduced latency, and access to fine-grained real-time data. Such models have been deployed for a variety of machine learning tasks, such as smart keyboard (AbdulRahman et al. 2020), personalized assistant services (Hao 2020), computer vision (Liu et al. 2020), healthcare (Rieke et al. 2020), and ranking (Hejazinia et al. 2022; Hartmann et al. 2019; Paulik et al. 2021).

At the same time, on the other hand, there are certain limitations that hinder the wide adoption of on-device AI models. Firstly, the limited computational and memory resources of client devices also restrict the size of the deployed models. As a result, the learning capacity and accuracy can be

significantly worse than the equivalent server-based models. Secondly, end-user devices might have limited access to large datasets or have the capacity to store and process features that require large embedding tables.

While on-device AI helps us ensure privacy, a key observation is that not all features might be sensitive, user-specific, or generated on-device. Examples include e-commerce item embeddings in a recommendation system, word embeddings of a large language model, ads-related features, etc. As such, training a small model entirely on-device might not be the optimal policy.

One promising approach to overcome these limitations is Split Learning (SL) (Gupta and Raskar 2018; Vepakomma, Balla, and Raskar 2020). Typically, a large machine learning model is divided into two parts: the bigger part resides on the server side (typically hosted by the model owner), and a smaller part can be executed on-device (typically hosted by the end-users). Larger models can then be collaboratively trained on both private (client) and non-private (server) features while limiting the information exchange between the involved parties.

During inference, the server initiates the forward pass utilizing all the server-side features. Large embedding tables and model architectures can be utilized at this stage. Only the activations of the *cut layer* are then shared with the end devices, typically a small vector. Each device continues the execution on its own sub-model, combining it with its own private features. Due to the limited capabilities, the client-side model is small, often only utilizing numerical features or categorical features with small cardinality. In this paper, we consider the most private scenario where the label is also private (e.g., the label represents a user purchase or a conversion after seeing an ad).

While split learning only considers two parties (e.g., ads publishers and advertisers), Federated Split Learning (FSL) allows us to train such models between a central party and millions of client devices (Thapa et al. 2022). In both cases, training the server-side model requires exchanging the gradients at the cut layer for each sample. Consequently, the returning cut-layer gradients might encode information that can reveal either private features and/or labels.

This paper provides insights into the potential risks of private data leakage during split model training. To achieve this, we introduce an extensive attack method that aims to

*This work is done while Xinchi Qiu was interning at Meta, Email: xq227@cam.ac.uk
Copyright © 2024, Association for the Advancement of Artificial Intelligence (www.aaai.org). All rights reserved.

reconstruct private information - features or labels - by exploiting diverse information sources at the cut layer, such as the model parameters, the activations, and gradients at the cut layer. Through our study, we aim to highlight the potential privacy risks associated with split learning by studying in which way features might be more sensitive to leakage. Finally, a significant part of the paper is devoted to studying how different strategies can help us mitigate these risks.

To sum up, in this work:

- We are the first to use an extensive and custom clustering-based attack method on SL. This method exploits diverse information sources, such as the model parameters, activations, and gradients at the cut layer, to reconstruct private information, including features or labels.
- We study how different mitigation strategies, such as label and gradient differential privacy (DP), can help us protect such on-device private features.
- Our results over three different datasets indicate that the gradients significantly improve the effectiveness of the attack methods when compared to the baselines. In all three datasets, an attacker is able to perfectly reconstruct labels and most features. However, adding a small amount of noise on the gradients at the cut layer (e.g., $\sigma = 0.01$) effectively mitigates this risk with a mere 0.01 drop in the model’s AUC.

2 Background and Related Work

Split Learning (SL) enables collaborative training of deep learning models among multiple parties without the need to share raw data. While Federated Learning (McMahan et al. 2017) can be utilized for such models, it may not always be practical. For instance, e-commerce and ad-ranking models often involve numerous sparse (categorical) and numerical features, requiring large machine learning models that can reach sizes of hundreds of gigabytes. Such models are typically too large to be trained on mobile devices (Qiu et al. 2022a; Horvath et al. 2021), whereas user-side features and labels (e.g., past purchases) might be too sensitive to collect on the server side.

In split learning (SL), the overall model is horizontally divided into two parts. The server handles the forward/backward passes of the first and larger portion of the model while keeping the last few layers to be trained with sensitive user-side data/features on the device. This division point in the model architecture is referred to as the *cut layer*. The server uses server-side features to perform a forward pass until the cut layer and then forward the intermediate representations to the respective clients. At each client, a smaller architecture processes the private features, which are then combined with the server-side representations. An overarching architecture is employed to make the final prediction. An example illustrating this process is depicted on the left side of Figure 1. During back-propagation, gradients are calculated from the last layer to the cut layer in a similar manner. The corresponding gradients are then sent back to the server to complete the server-side back-propagation. While no raw data are exchanged, these gradients might still encode private

information that can reveal either features and/or the ground truth labels that are stored on the devices.

Membership inference attacks aim at inferring whether a given sample was part of a model’s training set. Originally proposed in (Homer et al. 2008), it was popularized by the shadow models approach of Shokri et al. (Shokri et al. 2017). Follow-up work has shown that the membership signal can be derived from simple quantities, such as a low loss (Salem et al. 2018; Sablayrolles et al. 2019). Recent research has improved the performance of such attacks by comparing the loss to a calibrating term (Watson et al. 2021) or computing statistics on the distribution of the loss (Carlini et al. 2022).

Reconstruction attacks and attribute inference aim at reconstructing points from the training set given access to a trained model (Carlini et al. 2019), and to partial information about the sample in the case of attribute inference (Fredrikson et al. 2014; Yeom et al. 2018). Carlini et al. (Carlini et al. 2021) show that given access to a trained language model, an attacker is able to reconstruct verbatim samples with high precision (but low recall).

Attacks on Federated Learning. Recovering private features from gradients has gained growing interest in the privacy-preserving machine learning area. A popular method called Deep Leakage from Gradients (DLG) (Zhu, Liu, and Han 2019) has been developed to extract training data by using the shared model gradients. An improved version of DLG, iDLG (Zhao, Mopuri, and Bilen 2020), resulted in a more reliable approach to extracting accurate data and perfectly reconstructing the labels. However, these methods lack generalization on model architecture and weight distribution initialization (Wang et al. 2020). In (Geiping et al. 2020), an analytical approach has been developed to derive the inputs before a fully connected (FC) layer. (Fan et al. 2020) claimed that a convolutional layer can always be converted to an FC layer, but the gradients of the original convolutional layer are still different from the gradients of the converted FC layer, which impedes the data reconstruction. In (Yin et al. 2021), the authors developed GradInversion to recover images from noise based on given gradients. All related work assumes access to the gradient of all the *weights*; in this paper, we consider attacks given access only to gradients of the *activations* at the cut layer.

Differential Privacy (DP) One of the methods to mitigate the effectiveness of these attacks is DP (Dwork 2006). In the paper, we experiment with both DP-SGD (Abadi et al. 2016a) and Label DP (Ghazi et al. 2021a,b). Since SL requires the device and the server to exchange activations and gradients, it can potentially leak private label information (Hejazinia et al. 2022; Pasquini, Ateniese, and Bernaschi 2021). Differential privacy (Abadi et al. 2016b) constitutes a strong standard for privacy guarantees for algorithms on aggregate databases.

Definition 2.1. A randomized mechanism $\mathcal{M} : \mathcal{D} \rightarrow \mathcal{R}$ with domain \mathcal{D} and range \mathcal{R} satisfies (ϵ, δ) -differential privacy if for any two adjacent inputs $d, d' \in \mathcal{D}$ and for any subset of outputs $S \subseteq \mathcal{R}$ it holds that:

$$\Pr[\mathcal{M}(d) \in S] \leq e^\epsilon \Pr[\mathcal{M}(d') \in S] + \delta.$$

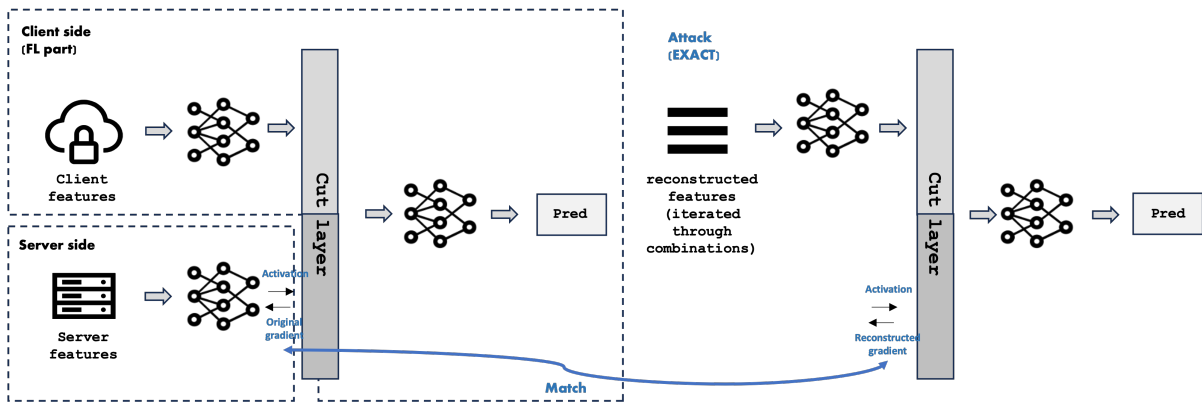


Figure 1: Illustration of SL (left) and our attack (right). During training, the server performs a forward pass until the cut later and then sends the intermediate representations to each client. This information and private features are used on-device to resume the computation. During the backward pass, the partial gradients returned might encode private client features or labels. Our attack uses these gradients to reconstruct the private features.

One of the most widely adopted methods to ensure DP is through DP-SGD (Abadi et al. 2016b), via norm clipping and adding noise (σ) to gradients. In our case, since only the gradients of the activations at the cut layer are shared directly from the client to the server, we only consider clipping and adding noise to this part of the whole gradient. In addition, the ϵ can be estimated through DP-accountant in various packages. There is a trade-off between model performance and model security, and carefully tuning the noise of DP is required to ensure that the trained model is effectively protected while maintaining a reasonable model performance (Kairouz et al. 2021).

On the other hand, Label DP is also based on a randomized response algorithm to improve the robustness of the training model. It is implemented when only labels need to be protected. It operates by randomly flipping the label based on the flipping probability (p) during training. The corresponding privacy budget ϵ can be estimated through the formula: $p = \frac{1}{e^\epsilon + 1}$.

3 Privacy and Split Learning

In this section, we present an extensive attack method for SL. We assume that clients have client-side private features that they would not want to share with any third party. Also, we consider that the ground-truth labels can also be private (i.e., only known to the clients) to study label leakage too. We consider the attack scenario where an honest-but-curious server follows the regular SL protocol but intends to recover clients' private data and the ground-truth labels based on the gradients of the cut layer. We design a custom and extensive attack method, termed *EXACT: Exhaustive Attack for Split Learning*. We use tabular datasets throughout the paper and experiments and will discuss the extension and future research later.

We consider a C class classification problem defined over a server feature space \mathcal{X}_{server} , a client feature space \mathcal{X}_{client} and a label space $\mathcal{Y} = [C]$, where $[C] = \{1, \dots, C\}$. We define F_{server} to be the server-side function, such that $F_{server} :$

$\mathcal{X}_{server} \rightarrow \mathbb{R}^d$, which outputs the server-side activations a_c . We also define the client-side $F_{client} : \mathcal{X}_{client} \times \mathbb{R}^d \rightarrow \mathcal{S}$, which maps the client feature space and the server's output to the probability simplex $\mathcal{S} = \{\mathbf{z} | \sum_{i=1}^L z_i = 1, z_i \geq 0, \forall i \in [C]\}$. Both F_{server} and F_{client} are parameterized over the hypothesis class $w = (w_{server}, w_{client})$, which is the weight of the neural network. $\mathcal{L}(\mathbf{w})$ is the loss function, and we assume the widely used cross-entropy loss.

In this way, the server's output (a_c) is the activation transmitted from the server to the client at the cut layer, and the weight of the cut layer is w_c . Also, the gradients transmitted from the client to the server are the gradient of the cut layer activations: $\partial\mathcal{L}/\partial a_c$. On the other hand, the gradients of the cut layer weight $\partial\mathcal{L}/\partial w_c$ stay on the client side to finish the back-propagation and allow the weights (weights on the clients-side, including the cut layer) to be updated, as shown on the left side of Figure 1.

Threat Model: We assume a strong attacker with access to the client-side model parameters during training. While we want to study cases where the attacker has fine-grained information, the attack model can be relaxed in cases where the secure aggregation is used, and only the final model parameters are known after the training is finished. In our scenario, we assume that an honest-but-curious server has knowledge of the server-side features, and the server-side and client-side models, which is a realistic assumption given the distributed setting of both SL and FSL. As a result, we assume that an adversary can compute the server-side outputs a_c for any server-side feature values, and with the input of client-side feature, the adversary can then obtain the corresponding cut-layer gradients ($\partial\mathcal{L}/\partial a_c$) from client-side. As $\partial\mathcal{L}/\partial a_c$ depends on the private features, the client-side architecture, and the output of the server a_c , we want to use all available information to reconstruct the private features (Figure 1).

3.1 Attack Method

assumes that the private features on the client side are either categorical or can be binned/clustered into a finite number

Algorithm 1: EXACT: Let f_1, \dots, f_N be the client-side private features; C be the number of classes for the task; a_c be the server output; $x(1, \dots, x_N, l)_i$ be the private features and label of the client i ; $\frac{\partial \mathcal{L}}{\partial a_c}$ be the gradient of cut layer activation that connected to the server; F_{client} be the model on the client side with p_{clt} be the client output; F_{server} be the model on the server side.

```

procedure EXACT
  Get  $\frac{\partial \mathcal{L}}{\partial a_c}$  ▷ Get the transmitted gradient
  Get server output  $a_c$  ▷ Get the server's output
   $L = f_1 \times f_2 \times \dots \times f_N \times L$  ▷ list of all combinations
  for  $i = 1, \dots, |L|$  do
     $L[i] = (x_1, \dots, x_N, l)_i$  ▷ iterate the  $i$ th combination
     $p_{clt} = F_{client}(a_c, (x_1, \dots, x_N, l)_i)$  ▷ Forward-prop on client model
     $d_i = \left| \frac{\partial \mathcal{L}_i}{\partial a_c} - \frac{\partial \mathcal{L}}{\partial a_c} \right|$  ▷ Compute the dist. between reconstructed and original gradient
  end for
   $p = \text{argmin}_i \{d_i : i = 1, \dots, |L|\}$  ▷ Get the index
  return  $L[p]$  ▷ Return the reconstructed features and label
end procedure

```

of categories. We then build a list L that contains all the possible configurations of client-side private features and labels. For a given sample, the adversary can calculate a_c and the gradient $\partial \mathcal{L}_i / \partial a_c$ for every possible private configuration $L[i]$. We then iterate all the configurations and then match the gradient $\partial \mathcal{L}_i / \partial a_c$ by choosing the configuration $L[i]$ that minimizes the distance to the true gradient $\partial \mathcal{L} / \partial a_c$ returned by the client. Here, we choose to use the L2 distance as the distance metric to compare the gradients. The details of the algorithm can be found in Algorithm 1.

Noting that in case the search space is growing with the number of features or categories to be attacked (i.e., many private features with thousands of categorical values), a heuristic approach or smart search methods can be used to speed up convergence to a given configuration. However, it is also worth mentioning that for the attack method, our priority concern is the attack performance for evaluation of the privacy leakage rather than speed. As a reference, in the datasets used here, we could successfully reconstruct features of a given sample within 16.8 seconds. Also, similar to many existing attack methods, such as DLG (Zhu, Liu, and Han 2019), iDLG (Zhao, Mopuri, and Bilen 2020), and GradInversion (Yin et al. 2021), our method *EXACT* reconstructs the private data via gradient matching. Unlike the previous methods, *EXACT* does not rely on optimization steps, which often involve second derivatives computations or carefully tuned regularization terms. By iterating through all possible possibilities, *EXACT* guarantee to reconstruct the most relevant private features without having convergence issues in the optimization steps.

4 Evaluation

4.1 Experimental Setup

We conducted comprehensive experiments on three different datasets, and the details of implementation can be found below. We conducted training in both SL and FSL ways. For

FSL, we simulate the federated environment by randomly allocating 16 samples for each client. All experiments are repeated three times.

Datasets: Experiments are conducted over three datasets: *Adult Income dataset* (Kohavi et al. 1996), *Bank Marketing dataset* (Moro, Laureano, and Cortez 2011), and *Taobao ad-display/click dataset* (Li et al. 2021). The Adult Income dataset is a classification dataset aiming to predict whether the income exceeds 50K a year based on census data. It contains 48,842 and 14 columns. The Bank Marketing dataset is related to the direct marketing campaigns of a Portuguese banking institution. It contains 45,211 rows and 18 columns ordered by date. We also conduct our experiment over a production scale ad-display/click dataset of Taobao (Li et al. 2021). The dataset contains 26 million interactions (click/non-click when an Ad was shown) and 847 thousand items across an 8-day period. We use 90% of the dataset as the training set and leave 10% as the testing set.

For the Adult Income and the Bank dataset, we randomly partition the features into server features and private client features. For the Taobao dataset, we keep the user-related features as private client features. It is worth noting that since the datasets are not pre-partitioned, our methods can work with any feature partitioned, which is shown separately in Section 4.4. We attack all the private features, and the particular private features for each dataset can be found in Table 32 and 4.

Model Architecture We deploy the state-of-the-art model, DeepFM, as the classification model (Li et al. 2021; Guo et al. 2017). We use a learning rate of 0.01 with Adagrad and binary cross entropy as the loss function. The default number of neurons for the DNN layer for the DeepFM is chosen to be (256,128). For the attack, we train the models in different scenarios in the SL and FSL fashion with the training set and then attack the private client features using the testing set that is not seen by the model before.

Baseline: We also implement two baselines to compare the attack performance. The baselines serve as guidance to show the extra information the gradient is leaking compared to our prior ability to reconstruct these private features using only server-side information. The first baseline is to reconstruct the client's features using the server's features. The second baseline is to use the server's output a_c to reconstruct the client's features. For both baselines, we use the K-nearest-neighbors algorithm (KNN), which is also a non-parametric method like our method. Since our method already outputs the configurations of the features that match the closest to the original gradient, there is no extra benefit of comparing with existing parametric or optimization-based methods.

DP: We implement both Label DP and DP as explained in Section 2 as mitigation and defense strategy for our attack. For Label DP, we implement flipping probability p of both 0.1 ($\epsilon = 2.2$) and 0.01 ($\epsilon = 4.6$). For DP, we implemented DP-SGD using clip norm C as half the gradient norm according to (Andrew et al. 2021) and noise multiplier 0.01.

4.2 Results

First of all, Table 1 shows the model performance for all three datasets in various setups and scenarios. As all three datasets are unbalanced in terms of classes, the table reports the AUC with or without DP noise. SL and FSL columns report the unmitigated training without DP. We also consider Label DP, DP, and a combination of Label DP and DP for the SL training. Both methods are explained in Section 2. SL and FSL report almost the same performance, which is reasonable, as both trainings are following per mini-batch steps. For Label DP, the table reports two different flipping probabilities. As we expected, with higher probability, the performance dropped for all datasets. For DP, since the noise added to the gradient is small, the degradation of the performance compared to the normal split training is also minimal. It is worth noting that the model performance (AUC), as shown in Table 1 for Taobao, is much lower than the other datasets, due to the fact that Taobao is a production scale and more difficult dataset to train with.

Then, we demonstrate the attack performance in detail in Table 2, 3, and 4. Since all features are not balanced, we choose to report the F1 score for our attack performance instead of accuracy.

The first thing to notice is that with both SL and FSL training for all datasets, the label can be reconstructed perfectly, which shows the importance of applying techniques such as label DP.

Also, for both FL and FSL, the attack performance on the private features for both adult income and bank marketing datasets are all above 0.95, implying accurate reconstructed performance for the attack in the unmitigated setting. As for the production scale dataset Taobao, some performance dropped to be around 0.80 but still shows good attack performance, which might be due to the fact that the model performance for Taobao is lower than the other two datasets.

As for Label DP, the attack accuracy is reported next to the F1 score in all three tables, which shows that the accuracy is exactly the same as the flipping probability. The attack performance for private features for the Label DP case is quite similar to the performance for the standard split training in all three datasets, showing that the flipping label does not provide enough protection for private features.

DP, on the other hand, has much more impact on the attack performance compared to Label DP. As we can see from Table 2, 3 and 4, the F1 scores significantly decrease for all private features and the Labels, with some of the F1 scores near 0, even with very small noise. For example, the attack performance for the Label for the Taobao dataset is 0 in Table 4 because the attack reconstructed all the labels to be label 0. It might be due to the fact that the dataset is extremely unbalanced, with only 5% of the total sample labeled as positive. As for the Age features in Table 4, the F1 score is extremely low since the attack accuracy is extremely low.

In addition, the tables also demonstrate the attack performance if we combine both Label DP and DP. As we expected, the performance for the combination will be more similar to the DP as DP has a significant impact on the attack performance, and all results show similar performance for the combined setup and the DP-only setup.

Lastly, for the baselines, the reconstructed performance for the baselines varies depending on the dataset. The baselines provide guidance to show the lower-bound information leakage from the server side, as we might see from the tables that the attack performance for the normal SL and training with Label DP outperforms the baselines for all datasets. However, there is no clear way to distinguish between the DP case and the baselines.

4.3 Model Architecture

We also conduct experiments to show that our results are not dependent on the particular model size, as shown in Table 5. We vary the DNN layers on the client side, as the gradient of the activation at the cut layer only depends on the model architecture on the client side, to see if model architecture can impact the attack performance. As we can see from the table, all SL training without mitigation demonstrates consistent performance across all private features, and the attack performances for the label are perfect. Similarly, for the DP performance, it all degrades to a similar level across all different model architectures indicating the effectiveness of DP on the attack.

4.4 Different Features

First, we conduct experiments to show that our results are not dependent on the selection of private features. The results are shown in Table 6. It demonstrates that our method can reconstruct the private features with unmitigated SL regardless of the partition of private features and the number of categories for each feature. If we only attack 1 private feature (Gender with 2 categories or Education with 16 categories), the reconstruction performance can be 100% regardless of the number of categories of the features. It is worth noticing that the attack performance drop below 0.5 if we consider the extreme case when we attack all categorical features, but it can still perfectly attack the ground truth label. Similar to the previous results, the attack performance degrades significantly if we incorporate DP. Also, if we attack all 7 features with DP, the label attack returns everything as label 0, which outputs the 0 F1 score, meaning that the gradient of the cut layer yields no useful information.

In addition, we also conduct experiments to investigate the attack effectiveness if we include non-relevant private features on the client side. ‘cms_group’ is the private feature that does not contribute to the model performance. With or without ‘cms_group’, testing AUC for the model are both 0.66, but as we can see from Table 7, adding the non-relevant features has an impact on the attack performance, especially for the unmitigated SL case.

4.5 Majority Vote

Furthermore, we also add a variation to our attack method. Instead of choosing the feature that derives the closest distance between the reconstructed gradient and the original gradient, like mentioned Algorithm 1, we return the k closest combination of reconstructed features and take the majority vote for each feature as the final reconstructed feature. Table 8 shows the results on the Adult dataset, with different values of k .

Table 1: Results (AUC) of model for each dataset on test-set in different scenarios.

Data	SL	FSL	Label DP		DP	Label DP & DP
			$p = 0.1$	$p = 0.01$	$\sigma = 0.01$	$p, \sigma = 0.01$
Bank	0.88±0.0024	0.88±0.0023	0.87±0.0039	0.88±0.0025	0.87±0.0003	0.87±0.0017
Adult	0.89±0.0033	0.89±0.0030	0.89±0.0037	0.89±0.0036	0.89±0.0034	0.89±0.0024
Taobao	0.66±0.0001	0.66±0.0001	0.62±0.0007	0.65±0.0002	0.65±0.0012	0.65±0.0013

Table 2: Results (F1 scores) of the feature reconstruction attack on test-set, compared with the baselines on the Adult Income dataset. The number of categories for each feature is shown in the bracket next to each feature name. For Label in Label DP, the accuracy is reported in the bracket

Features (Num)	SL	FSL	Label DP		DP	Comb.	Baseline	
			$p = 0.1$	$p = 0.01$			features	output
Gender(2)	0.9977	0.9990	0.9996	0.9996	0.3652	0.3430	0.7909	0.7729
Race(5)	0.9878	0.9888	0.9777	0.9711	0.1119	0.0808	0.3344	0.2789
Relationship (6)	0.9952	0.9957	0.9860	0.9974	0.0828	0.0756	0.1998	0.2917
Marital(7)	0.9912	0.9526	0.9794	0.9903	0.1424	0.1241	0.1736	0.2570
Label(2)	1	1	0.80(0.90)	0.98(0.99)	0.5497	0.5558	0.3850	0.5234

Table 3: Results (F1 scores) of the feature reconstruction attack on test-set, compared with the baselines on the Bank Marketing dataset. The number of categories for each feature is shown in the bracket next to each feature name. For Label in Label DP, the accuracy is reported in the bracket

Features (Num)	SL	FSL	Label DP		DP	Comb.	Baseline	
			$p = 0.1$	$p = 0.01$			features	output
Martial(3)	0.9578	0.9712	0.9877	0.9800	0.2157	0.3037	0.3229	0.4343
Job(12)	0.9490	0.9515	0.9780	0.9632	0.0182	0.0188	0.0966	0.1697
Education(4)	0.9499	0.9622	0.9782	0.9795	0.1898	0.1280	0.2499	0.2845
Housing(2)	0.9835	0.9808	0.9941	0.9911	0.5975	0.5670	0.7112	0.7584
Loan(2)	0.9332	0.9418	0.9737	0.9621	0.2656	0.2666	0.0909	0.1310
Contact(3)	0.9770	0.9716	0.9886	0.9841	0.2683	0.3859	0.5406	0.6102
Label(2)	1	1	0.6893 (0.90)	0.9587(0.99)	0.3929	0.3682	0.3504	0.4275

Table 4: Results (F1 scores) of the feature reconstruction attack on test-set, compared with the baselines on the Taobao dataset. The number of categories for each feature is shown in the bracket next to each feature name. For Label in Label DP, the accuracy is reported in the brackets. 0 F1 scores indicate that the attacker reconstructs all the label as 0 in all cases.

Features (Num)	SL	FSL	Label DP		DP	Comb.	Baseline	
			$p = 0.1$	$p = 0.01$			features	output
Age(7)	0.8284	0.8135	0.8470	0.7852	0.0464	0.0001	0.2643	0.1660
P-value(3)	0.8880	0.8499	0.9178	0.8607	0.0256	0.0256	0.4022	0.3280
Shopping(3)	0.9034	0.8582	0.9321	0.8583	0.3065	0.3062	0.4503	0.3281
Occupation(2)	0.8036	0.8562	0.8931	0.6523	0.1031	0.0975	0.1151	0.0228
Label(2)	1	1	0.4832(0.90)	0.9076(0.99)	0	0	0.0066	0.0326

Table 5: Results (F1 scores) of the feature reconstruction attack on test-set on the Adult Income dataset with various architecture on the client-side model.

Features (Num)	SL			DP		
	(256,128)	(64,32)	(32,16)	(256,128)	(64,32)	(32,16)
Gender(2)	0.9977	0.9979	0.9987	0.3652	0.3330	0.1631
Race(5)	0.9878	0.9692	0.9830	0.1119	0.2010	0.0671
Relation(6)	0.9952	0.9894	0.9896	0.0828	0.0831	0.0674
Marital(7)	0.9912	0.9436	0.9789	0.1424	0.1233	0.1054
Label(2)	1	1	1	0.5497	0.4855	0.4554

The results show that, as k increases, the attack performance drop for both unmitigated SL training and training with DP, which shows that the attack performance is highly sensitive to the variation of gradient, and it has to match exactly to generate good reconstruction performance.

5 Discussion

Feature reconstruction: Our experiments indicate that the gradients required for SL from the client to the server can be used to reconstruct private features and labels. Compared to our baseline ability to predict the private features from the public features, the gradients significantly improve the

Table 6: Results (F1 scores) of the feature reconstruction attack on test-set on the Adult Income dataset with various sets of private features. Feature 'Occu' is short for 'Occupation', 'Work' for 'Workclass', and 'Edu' for 'Education'. For the F1 score, 1 means that it is perfectly equal to 1 and 1.00 means it is rounded up to 1.00. '-' means that the feature is not considered as a private feature, so it is not attacked.

Features	SL	DP	SL	DP	SL	DP	SL	DP	SL	DP	SL	DP	SL	DP	SL	DP
Gender(2)	1	0.36	1	0.33	1.00	0.26	1.00	0.36	0.97	0.24	0.90	0.21	0.81	0.51	-	-
Race(3)	-	-	1	0.33	1	0.08	1.00	0.12	0.77	0.10	0.46	0.09	0.25	0.15	-	-
Marital(7)	-	-	-	-	1.00	0.14	1.00	0.09	0.74	0.12	0.50	0.09	0.25	0.07	-	-
Relation(6)	-	-	-	-	-	-	-	0.99	0.14	0.92	0.07	0.70	0.09	0.52	0.04	-
Occu.(15)	-	-	-	-	-	-	-	-	0.83	0.05	0.62	0.04	0.39	0.08	-	-
Work(9)	-	-	-	-	-	-	-	-	-	-	0.52	0.05	0.26	0.10	-	-
Edu.(16)	-	-	-	-	-	-	-	-	-	-	-	-	0.32	0.03	1	0.08
Label(2)	1	0.62	1	0.77	1	0.55	1	0.55	1	0.39	1	0.32	1	0	1	0.62
															1	0.66

Table 7: Results (F1 scores) of the feature reconstruction attack on test-set on the Taobao dataset with private features with or without 'cms group'. 0 F1 scores indicate that the attacker reconstructs all the labels as 0 in all cases.

Features (Num)	SL	DP	SL	DP
		$\sigma = 0.01$		$\sigma = 0.01$
CMS Group (12)	0.0584	0.0001	-	-
Age(7)	0.6884	0.0119	0.8284	0.0464
P-value(3)	0.5792	0.0246	0.8880	0.0256
Shopping(3)	0.6635	0.3076	0.9034	0.3065
Occupation(2)	0.3890	0.1032	0.8562	0.1031
Label(2)	1	0	1	0

Table 8: Results (F1 scores) of the feature reconstruction attack on test-set on the Adult Income dataset with various k-value for the majority vote.

Features (Num)	SL			DP		
	k = 1	k = 5	k = 10	k = 1	k = 5	k = 10
Gender(2)	0.9977	0.8231	0.7760	0.3652	0.3269	0.2761
Race(5)	0.9878	0.2359	0.0543	0.1119	0.0786	0.0626
Relationship(6)	0.9952	0.5723	0.3777	0.0828	0.0759	0.0760
Marital(7)	0.9912	0.4956	0.5153	0.1424	0.1348	0.1375
Label(2)	1	1	0.9995	0.5479	0.5351	0.5029

effectiveness of the attack method in all three datasets we experimented with.

Effectiveness of DP noise: We have studied adding a wide range of DP noise, and we observe that even a small amount is enough to mitigate the reconstruction attack while allowing the model to reach similar training performance. This is because we only need to add noise on the cut-layer returned gradients. Note that in the Federated Split Learning setting, global DP is also added on the client-side models too before releasing outside the secure aggregator to ensure that the client-side weights do not encode any private information.

Studying different architectures: While we mostly focused on a typical (fully connected) DNN architecture on the client side, in future work, we want to examine further how different architectures (e.g., CNNs, RNNs, etc) can affect the ability to reconstruct private features and the sensitivity to these DP mitigation strategies.

Speeding up the attack: In our attack, we need to compare the returned gradient with every possible gradient that can result from different configurations of private features. Obviously, the wall clock time of the search depends largely on the search space, and it will significantly increase if the number of categories to search over is big. For example, for our dataset, on average, we require 20 milliseconds to finish one forward and backward pass. In this case, for the Adult dataset, each reconstruction goes over 840 times, which amounts to 16.8 seconds for each sample reconstruction. There are multiple heuristic-based grid-search techniques that can help us accelerate this search, including subset searching, gradient descent, Bayesian search (Chang 2021), and so on.

Split learning and Federated Learning: Our initial experiments indicate that these findings also hold in Federated Split Learning (FSL), where there is more than one client with private features participating in training. However, in our scenarios, we randomly allocate samples to each client, which represents the Independent and identically data distribution (IID) scenario. We plan to study how non-IID can cause extra difficulties either in attacking FSL (Li et al. 2020; Karimireddy et al. 2020; Qiu et al. 2022b).

Extending to other attacks: In this work, we focused on reconstruction attacks on categorical features. However, *EXACT* can easily be extended to membership inference attacks if we binned/clustered private features into a finite number of categories. In this case, our method would be able to infer if the particular feature is from a particular cluster.

6 Conclusion

In this paper, we study the potential leakage of private features and labels during split model training. We introduce a custom and extensive feature reconstruction method and apply it to various datasets. Our results indicate that the exchanged gradients do encode private information, allowing the adversary to perfectly reconstruct labels and reconstruct private features with excellent performance. We then examine how mitigation strategies such as DP-SGD and Label DP can be used to successfully mitigate these risks without affecting the training quality. As in this work, we focused on tabular data, and we would like to expand on other tasks, such as image, text, audio processing, and other model architectures in future works.

References

- Abadi, M.; Chu, A.; Goodfellow, I.; McMahan, H. B.; Mironov, I.; Talwar, K.; and Zhang, L. 2016a. Deep learning with differential privacy. In *Proceedings of the 2016 ACM SIGSAC conference on computer and communications security*, 308–318.
- Abadi, M.; Chu, A.; Goodfellow, I.; McMahan, H. B.; Mironov, I.; Talwar, K.; and Zhang, L. 2016b. Deep learning with differential privacy. In *Proceedings of the 2016 ACM SIGSAC conference on computer and communications security*, 308–318.
- AbdulRahman, S.; Tout, H.; Ould-Slimane, H.; Mourad, A.; Talhi, C.; and Guizani, M. 2020. A survey on federated learning: The journey from centralized to distributed on-site learning and beyond. *IEEE Internet of Things Journal*, 8(7): 5476–5497.
- Andrew, G.; Thakkar, O.; McMahan, B.; and Ramaswamy, S. 2021. Differentially private learning with adaptive clipping. *Advances in Neural Information Processing Systems*, 34: 17455–17466.
- Carlini, N.; Chien, S.; Nasr, M.; Song, S.; Terzis, A.; and Tramer, F. 2022. Membership inference attacks from first principles. In *2022 IEEE Symposium on Security and Privacy (SP)*, 1897–1914. IEEE.
- Carlini, N.; Liu, C.; Erlingsson, Ú.; Kos, J.; and Song, D. 2019. The secret sharer: Evaluating and testing unintended memorization in neural networks. In *28th USENIX Security Symposium (USENIX Security 19)*, 267–284.
- Carlini, N.; Tramer, F.; Wallace, E.; Jagielski, M.; Herbert-Voss, A.; Lee, K.; Roberts, A.; Brown, T. B.; Song, D.; Erlingsson, U.; et al. 2021. Extracting Training Data from Large Language Models. In *USENIX Security Symposium*, volume 6.
- Chang, D. T. 2021. Bayesian Hyperparameter Optimization with BoTorch, GPyTorch and Ax. arXiv:1912.05686.
- Dwork, C. 2006. Differential privacy. In *Automata, Languages and Programming: 33rd International Colloquium, ICALP 2006, Venice, Italy, July 10-14, 2006, Proceedings, Part II 33*, 1–12. Springer.
- Fan, L.; Ng, K. W.; Ju, C.; Zhang, T.; Liu, C.; Chan, C. S.; and Yang, Q. 2020. Rethinking privacy preserving deep learning: How to evaluate and thwart privacy attacks. *Federated Learning: Privacy and Incentive*, 32–50.
- Fredrikson, M.; Lantz, E.; Jha, S.; Lin, S.; Page, D.; and Ristenpart, T. 2014. Privacy in pharmacogenetics: An {End-to-End} case study of personalized warfarin dosing. In *23rd USENIX Security Symposium (USENIX Security 14)*, 17–32.
- Geiping, J.; Bauermeister, H.; Dröge, H.; and Moeller, M. 2020. Inverting gradients-how easy is it to break privacy in federated learning? *Advances in Neural Information Processing Systems*, 33: 16937–16947.
- Ghazi, B.; Golowich, N.; Kumar, R.; Manurangsi, P.; and Zhang, C. 2021a. Deep learning with label differential privacy. *Advances in neural information processing systems*, 34: 27131–27145.
- Ghazi, B.; Golowich, N.; Kumar, R.; Manurangsi, P.; and Zhang, C. 2021b. Deep learning with label differential privacy. *Advances in neural information processing systems*, 34: 27131–27145.
- Guo, H.; Tang, R.; Ye, Y.; Li, Z.; and He, X. 2017. DeepFM: a factorization-machine based neural network for CTR prediction. *arXiv preprint arXiv:1703.04247*.
- Gupta, O.; and Raskar, R. 2018. Distributed learning of deep neural network over multiple agents. *Journal of Network and Computer Applications*, 116: 1–8.
- Hao, K. 2020. How Apple personalizes Siri without hoovering up your data. *Technology Review*.
- Hartmann, F.; Suh, S.; Komarzewski, A.; Smith, T. D.; and Segall, I. 2019. Federated learning for ranking browser history suggestions. *arXiv preprint arXiv:1911.11807*.
- Hejazinia, M.; Huba, D.; Leontiadis, I.; Maeng, K.; Malek, M.; Melis, L.; Mironov, I.; Nasr, M.; Wang, K.; and Wu, C.-J. 2022. Fel: High capacity learning for recommendation and ranking via federated ensemble learning. *arXiv preprint arXiv:2206.03852*.
- Homer, N.; Szelinger, S.; Redman, M.; Duggan, D.; Tembe, W.; Muehling, J.; Pearson, J. V.; Stephan, D. A.; Nelson, S. F.; and Craig, D. W. 2008. Resolving individuals contributing trace amounts of DNA to highly complex mixtures using high-density SNP genotyping microarrays. *PLoS genetics*, 4(8): e1000167.
- Horvath, S.; Laskaridis, S.; Almeida, M.; Leontiadis, I.; Venieris, S.; and Lane, N. 2021. Fjord: Fair and accurate federated learning under heterogeneous targets with ordered dropout. *Advances in Neural Information Processing Systems*, 34: 12876–12889.
- Kairouz, P.; McMahan, H. B.; Avent, B.; Bellet, A.; Bennis, M.; Bhagoji, A. N.; Bonawitz, K.; Charles, Z.; Cormode, G.; Cummings, R.; et al. 2021. Advances and open problems in federated learning. *Foundations and Trends® in Machine Learning*, 14(1–2): 1–210.
- Karimireddy, S. P.; Kale, S.; Mohri, M.; Reddi, S.; Stich, S.; and Suresh, A. T. 2020. SCAFFOLD: Stochastic Controlled Averaging for Federated Learning. In *Proceedings of the 37th International Conference on Machine Learning*. PMLR.
- Kohavi, R.; et al. 1996. Scaling up the accuracy of naive-bayes classifiers: A decision-tree hybrid. In *Kdd*, volume 96, 202–207.
- Li, L.; Hong, J.; Min, S.; and Xue, Y. 2021. A Novel CTR Prediction Model Based On DeepFM For Taobao Data. In *2021 IEEE International Conference on Artificial Intelligence and Industrial Design (AIID)*, 184–187. IEEE.
- Li, T.; Sahu, A. K.; Zaheer, M.; Sanjabi, M.; Talwalkar, A.; and Smith, V. 2020. Federated optimization in heterogeneous networks. *Proceedings of Machine Learning and Systems*, 2: 429–450.
- Liu, Y.; Huang, A.; Luo, Y.; Huang, H.; Liu, Y.; Chen, Y.; Feng, L.; Chen, T.; Yu, H.; and Yang, Q. 2020. Fedvision: An online visual object detection platform powered by federated learning. In *Proceedings of the AAAI Conference on Artificial Intelligence*, volume 34, 13172–13179.

- McMahan, B.; Moore, E.; Ramage, D.; Hampson, S.; and y Arcas, B. A. 2017. Communication-efficient learning of deep networks from decentralized data. In *Artificial intelligence and statistics*. PMLR.
- Moro, S.; Laureano, R.; and Cortez, P. 2011. Using data mining for bank direct marketing: An application of the crispdm methodology.
- Pasquini, D.; Ateniese, G.; and Bernaschi, M. 2021. Unleashing the tiger: Inference attacks on split learning. In *Proceedings of the 2021 ACM SIGSAC Conference on Computer and Communications Security*, 2113–2129.
- Paulik, M.; Seigel, M.; Mason, H.; Telaar, D.; Kluijvers, J.; van Dalen, R.; Lau, C. W.; Carlson, L.; Granqvist, F.; Vandeveld, C.; et al. 2021. Federated evaluation and tuning for on-device personalization: System design & applications. *arXiv preprint arXiv:2102.08503*.
- Qiu, X.; Fernandez-Marques, J.; Gusmao, P. P.; Gao, Y.; Parcollet, T.; and Lane, N. D. 2022a. ZeroFL: Efficient on-device training for federated learning with local sparsity. *arXiv preprint arXiv:2208.02507*.
- Qiu, X.; Fernandez-Marques, J.; Gusmao, P. P.; Gao, Y.; Parcollet, T.; and Lane, N. D. 2022b. Zerofl: Efficient on-device training for federated learning with local sparsity. *arXiv preprint arXiv:2208.02507*.
- Rieke, N.; Hancox, J.; Li, W.; Milletari, F.; Roth, H. R.; Albarqouni, S.; Bakas, S.; Galtier, M. N.; Landman, B. A.; Maier-Hein, K.; et al. 2020. The future of digital health with federated learning. *NPJ digital medicine*, 3(1): 119.
- Sablayrolles, A.; Douze, M.; Schmid, C.; Ollivier, Y.; and Jégou, H. 2019. White-box vs black-box: Bayes optimal strategies for membership inference. In *International Conference on Machine Learning*, 5558–5567. PMLR.
- Salem, A.; Zhang, Y.; Humbert, M.; Berrang, P.; Fritz, M.; and Backes, M. 2018. MI-leaks: Model and data independent membership inference attacks and defenses on machine learning models. *arXiv preprint arXiv:1806.01246*.
- Shokri, R.; Stronati, M.; Song, C.; and Shmatikov, V. 2017. Membership inference attacks against machine learning models. In *2017 IEEE symposium on security and privacy (SP)*, 3–18. IEEE.
- Thapa, C.; Arachchige, P. C. M.; Camtepe, S.; and Sun, L. 2022. Splitfed: When federated learning meets split learning. In *Proceedings of the AAAI Conference on Artificial Intelligence*, volume 36, 8485–8493.
- Vepakomma, P.; Balla, J.; and Raskar, R. 2020. Splintering with distributions: A stochastic decoy scheme for private computation. *arXiv preprint arXiv:2007.02719*.
- Wang, Y.; Deng, J.; Guo, D.; Wang, C.; Meng, X.; Liu, H.; Ding, C.; and Rajasekaran, S. 2020. Sapag: A self-adaptive privacy attack from gradients. *arXiv preprint arXiv:2009.06228*.
- Watson, L.; Guo, C.; Cormode, G.; and Sablayrolles, A. 2021. On the importance of difficulty calibration in membership inference attacks. *arXiv preprint arXiv:2111.08440*.
- Yeom, S.; Giacomelli, I.; Fredrikson, M.; and Jha, S. 2018. Privacy risk in machine learning: Analyzing the connection to overfitting. In *2018 IEEE 31st computer security foundations symposium (CSF)*, 268–282. IEEE.
- Yin, H.; Mallya, A.; Vahdat, A.; Alvarez, J. M.; Kautz, J.; and Molchanov, P. 2021. See through gradients: Image batch recovery via gradinversion. In *Proceedings of the IEEE/CVF Conference on Computer Vision and Pattern Recognition*, 16337–16346.
- Zhao, B.; Mopuri, K. R.; and Bilen, H. 2020. idlg: Improved deep leakage from gradients. *arXiv preprint arXiv:2001.02610*.
- Zhu, L.; Liu, Z.; and Han, S. 2019. Deep leakage from gradients. *Advances in neural information processing systems*, 32.